0090-9556/10/3810-1740–1746$20.00
DRUG METABOLISM AND DISPOSITION
DMD 38:1740–1746, 2010

Vol. 38, No. 10
34025/3628417
*Printed in U.S.A.*



# Significance and Regional Dependency of Peptide Transporter (PEPT) 1 in the Intestinal Permeability of Glycylsarcosine: In Situ Single-Pass Perfusion Studies in Wild-Type and *Pept1* Knockout Mice

Dilara Jappar, Shu-Pei Wu, Yongjun Hu, and David E. Smith

*Department of Pharmaceutical Sciences, College of Pharmacy, University of Michigan, Ann Arbor, Michigan*

Received April 19, 2010; accepted July 21, 2010

**ABSTRACT:**

**The purpose of this study was to evaluate the role, relevance, and regional dependence of peptide transporter (PEPT) 1 expression and function in mouse intestines using the model dipeptide glycylsarcosine (GlySar). After isolating specific intestinal segments, in situ single-pass perfusions were performed in wild-type and *Pept1* knockout mice. The permeability of [$^3$H]GlySar was measured as a function of perfusate pH, dipeptide concentration, potential inhibitors, and intestinal segment, along with PEPT1 mRNA and protein. We found the permeability of GlySar to be saturable ($K_m$ = 5.7 mM), pH-dependent (maximal value at pH 5.5), and specific for PEPT1; other peptide transporters, such as PHT1 and PHT2, were not involved, as judged by the lack of GlySar inhibition by excess concentrations of histidine. GlySar permeabilities were comparable in the duodenum and jejunum of wild-type mice but were much larger than that in ileum (approximately 2-fold). A PEPT1-mediated permeability was not observed for GlySar in the colon of wild-type mice (<10% residual uptake compared to proximal small intestine). Moreover, GlySar permeabilities were very low and not different in the duodenum, jejunum, ileum, and colon of *Pept1* knockout mice. Functional activity of intestinal PEPT1 was confirmed by real-time polymerase chain reaction and immunoblot analyses. Our findings suggest that a loss of PEPT1 activity (e.g., due to polymorphisms, disease, or drug interactions) should have a major effect in reducing the intestinal absorption of di-/tripeptides, peptidomimetics, and peptide-like drugs.**

## Introduction

In the gastrointestinal lumen, proteins are converted into large peptides by gastric and pancreatic proteases, which subsequently undergo further hydrolysis into small peptides (80%) and free amino acids (20%) by various peptidases in the brush border membrane of intestinal epithelia (Ganapathy et al., 2006). The final end products of protein digestion are absorbed into the enterocytes predominantly in the form of di-/tripeptides as opposed to free amino acids. Peptide transporter (PEPT) 1, a proton-coupled oligopeptide transporter (POT) with high capacity and low affinity, is believed to be the primary mechanism by which these small peptides enter the cell. Once inside the enterocyte, the majority of di-/tripeptides undergo further hydrolysis into their constituent amino acids by cytoplasmic peptidases and exit the epithelial cells by a distinct family of basolateral amino acid transporters. Those small peptides that are resistant to cytoplasmic peptidases may exit the enterocytes intact by crossing the basolateral membrane via a peptide transporter that has yet to be cloned.

This work was supported by the National Institutes of Health National Institute of General Medical Sciences [Grant R01-GM035498] (to D.E.S.).

Article, publication date, and citation information can be found at http://dmd.aspetjournals.org.

doi:10.1124/dmd.110.034025.

The POTs are membrane proteins that are responsible for translocating di-/tripeptides across biological membranes via an inwardly directed proton gradient and negative membrane potential (Rubio-Aliaga and Daniel, 2002; Daniel and Rubio-Aliaga, 2003; Herrera-Ruiz and Knipp, 2003; Daniel and Kottra, 2004). Thus far, four members of the POT family, specifically PEPT1 (SLC15A1), PEPT2 (SLC15A2), PHT1 (SLCA4), and PHT2 (SLCA3), have been cloned in mammals. In the intestine, PEPT1 functions at the apical membrane by mediating the electrogenic uphill transport of substrates and downhill transport of protons into epithelial cells (i.e., tertiary-active carrier). The driving force for this proton gradient is established by an apical $Na^+/H^+$ antiporter (i.e., secondary-active carrier), whereas the driving force for the inwardly directed sodium gradient is established by $Na^+/K^+$-ATPase, located at the basolateral membrane of intestinal epithelia (i.e., primary-active carrier). In addition to the nutritional role of absorbing nitrogen in the form of di-/tripeptides, PEPT1 transports a number of peptide-like therapeutic agents such as $\beta$-lactam antibiotics, angiotensin-converting enzyme inhibitors, renin inhibitors, bestatin, and the antiviral prodrug valacyclovir (Brandsch et al., 2008; Rubio-Aliaga and Daniel, 2008). Due to its broad substrate specificity and high capacity, PEPT1 is considered an attractive target for drug delivery strategies aimed at improving the bioavailability of poorly permeable drugs.

**ABBREVIATIONS:** PEPT, peptide transporter; POT, proton-coupled oligopeptide transporter; GlySar, glycylsarcosine; PCR, polymerase chain reaction; HRP, horseradish peroxidase; $P_{eff}$, effective permeability; PHT, peptide/histidine transporter; DMA, dimethylamiloride.

PEPT1 is the most extensively studied transporter among the POT members because of its physiological and pharmacological importance in the absorption of di-/tripeptides and peptide-like drugs from small intestine. However, most of the previous information regarding PEPT1 structure-function and significance was obtained from in vitro studies such as brush border membrane vesicles, cell cultures, and Xenopus oocytes, all of which use nonphysiological conditions that lack blood flow. It should also be appreciated that other POT family members are expressed in the intestine. For example, PEPT2 is found in glial cells and in tissue-resident macrophages of the enteric nervous system (Rühl et al., 2005). Moreover, the peptide/histidine transporters PHT1 and PHT2 have been found in intestinal tissue segments (Herrera-Ruiz et al., 2001), and immunohistochemical analyses have indicated that PHT1 is expressed in the villous epithelium of small intestine (Bhardwaj et al., 2006). However, the functional significance of PEPT2, PHT1, and PHT2 in the intestinal absorption of peptides/mimetics and peptide-like drugs is uncertain.

Heterogeneity has been observed in the intestinal expression of PEPT1 in mice and humans. Immunolocalization studies demonstrated that PEPT1 was expressed in the apical membrane of enterocytes in the small intestine (i.e., duodenum, jejunum, and ileum) of both species with little or no expression in normal colon (Walker et al., 1998; Groneberg et al., 2001). Whether PEPT1 activity agrees with its expression levels in various intestinal segments is still unknown. This heterogeneity, along with the existence of multiple peptide transport systems with overlapping substrate specificity, makes it difficult, if not impossible, to define the function and significance of a single specific gene product.

A recent article by Hu et al. (2008) described for the first time the development of *Pept1* null mice and their preliminary validation and phenotypic analysis in intestine. However, this study was limited in that the functional activity of glycylsarcosine (GlySar) was examined at only one concentration and pH value, and only in jejunal tissue. As a result, the objective of the current study was to define the significance and regional dependence of PEPT1 in the intestinal permeability of GlySar in wild-type and *Pept1* knockout mice. Using an in situ single-pass perfusion method, radiolabeled GlySar was studied as a function of perfusate pH, dipeptide concentration, potential inhibitors, and regional segment (i.e., duodenum, jejunum, ileum, and colon). The intestinal expression of PEPT1 mRNA and protein was also evaluated in these segments.

## Materials and Methods

**Animals.** Mouse studies were carried out in accordance with the Guide for the Care and Use of Laboratory Animals as adopted and promulgated by the U.S. National Institutes of Health (Institute of Laboratory Animal Resources, 1996). Gender-matched 8- to 10-week-old P*ept1*(+/+) (wild-type) and *Pept1*(−/−) (knockout) mice were used for all experiments. The mice were kept in a temperature-controlled environment with 12-h light/dark cycles and received a standard diet and water ad libitum (Unit for Laboratory Animal Medicine, University of Michigan, Ann Arbor, MI).

**Chemicals.** [$^3$H]GlySar (0.5 Ci/mmol) was purchased from Moravek Biochemicals and Radiochemicals (Brea, CA), and [$^{14}$C]PEG-4000 (1.5 mCi/g) was purchased from American Radiolabeled Compounds (St. Louis, MO). Unlabeled PEG-4000 was obtained from Mallinckrodt Baker, Inc. (Phillipsburg, NJ). Acyclovir and valacyclovir were generous gifts from GlaxoSmithKline (Research Triangle Park, NC). All other chemicals were acquired from Sigma-Aldrich (St. Louis, MO).

**In Situ Single-Pass Intestinal Perfusion.** Intestinal perfusion experiments were performed on wild-type and *Pept1* knockout mice according to methods described previously (Adachi et al., 2003; Hu et al., 2008). In brief, animals were fasted overnight with free access to water before each experiment. After anesthesia with sodium pentobarbital (40–60 mg/kg i.p.), surgery was performed on each animal while lying on top of a heating pad to maintain the body temperature. Isopropyl alcohol was used to sterilize the abdominal area, and a 1.5-cm midline incision was made longitudinally to expose the small intestine. An 8-cm segment of proximal jejunum was isolated (i.e., ~2 cm distal to the ligament of Treitz), and incisions were then made at the proximal and distal ends. Glass cannulas (2.0 mm outer diameter), attached to Tygon tubing, were inserted at each end of the jejunal segment and secured in place with silk sutures. After cannulations, the isolated intestinal segment was covered with saline-wetted gauze and parafilm to prevent dehydration of the tissue. The animals were then transferred to a temperature-controlled Plexiglas perfusion chamber (31°C) to maintain body temperature during the perfusion experiment. The inlet tubing was connected to a 10-ml syringe placed on a perfusion pump (model 22; Harvard Apparatus, South Natick, MA), and the outlet tubing was placed in a collection vial.

The perfusate (pH 6.5) contained 10 mM MES, 135 mM NaCl, 5 mM KCl, 10 $\mu$M [$^3$H]GlySar, and 0.01% (w/v) [$^{14}$C]PEG-4000, in the absence and presence of potential inhibitors, which flowed through the proximal jejunal segment at a rate of 0.1 ml/min. Exiting perfusate was collected every 10 min for 90 min. A 100-$\mu$l aliquot of perfusate was added to 5.5 ml of scintillation cocktail (Ecolite; MP Biomedicals, Solon, OH), and the samples were analyzed with a dual-channel liquid scintillation counter (Beckman LS 6000 SC; Beckman Coulter Inc., Fullerton, CA). [$^3$H]GlySar, a hydrolysis-resistant dipeptide, was added to perfusate as a model substrate, and [$^{14}$C]PEG-4000 was added to perfusate as a nonabsorbable marker to measure water flux. For pH-dependent analyses, different combinations of 10 mM MES/Tris or HEPES/Tris were used in perfusate to adjust pH values between 5.0 and 7.4, with osmolarity being held constant.

**Regional Intestinal Permeability.** Simultaneous perfusions, as described previously in rats (Jeong et al., 2004), were adapted for our studies in wild-type and *Pept1* knockout mice. Before cannulations of different intestinal segments, the common bile duct was ligated by silk suture. A 2-cm segment of duodenum (i.e., ~0.25 cm distal to the pyloric sphincter), 8-cm segment of jejunum (i.e., ~2 cm distal to the ligament of Treitz), 6-cm segment of ileum (i.e., ~1 cm proximal to the cecum), and 3-cm segment of colon (i.e., ~ 0.5 cm distal to the cecum) were then perfused as described above for jejunum alone.

**TaqMan Real-Time Polymerase Chain Reaction Analyses.** Quantification of PEPT1 transcripts were carried out in different segments of small and large intestines from wild-type mice using the 7300 Real-Time PCR System (Applied Biosystems, Foster City, CA) (Hu et al., 2008). The total RNA was isolated using an RNeasy Plus Mini Kit (QIAGEN, Valencia, CA) and then reverse-transcribed. Primers and probes were designed with Primer Express 3.0 software (Applied Biosystems), and all the primers, probes, and standard DNA were synthesized by Integrated DNA Technologies, Inc. (Coralville, IA). The forward and reverse primers and probe for PEPT1 were CTTGGAGCCACCACAATGG, ACAGAATTCATTGACCACGATGA, and 5′-/56-FAM/-TTGCTTCGGTTACCCGTTGAGCATCT-/36-TAMSp/-3′, respectively. The forward and reverse primers and probe for glyceraldehyde 3-phosphate dehydrogenase were GAGACAGCCGCATCTTCTTGT, CACACCGACCTTCACCATTTT and 5′-/56-JOE/-CAGTGCCAGCCTCGTCCCGTAGA-/36-TAMSp/-3′, respectively. The thermal profile was 1 cycle at 50°C for 2 min, 1 cycle at 95°C for 10 min, 40 cycles at 95°C for 15 s, and 60°C for 1 min. The absolute amount of PEPT1 transcripts was calculated automatically based on the standard curve and then normalized by glyceraldehyde 3-phosphate dehydrogenase transcript expression.

**Immunoblot Analyses.** Mucosa was scraped off the different segments of small and large intestine from wild-type mice and homogenized in 2 ml of Nonidet P40-lysis buffer (50 mM Tris-HCl, 150 mM NaCl, 1% Nonidet P40, proteinase inhibitor cocktail, pH 8.0). The homogenate was then centrifuged at 15,000*g* for 5 min at 4°C, and the suspension was sonicated for 10 pulses at one-half strength, followed by a second centrifugation at 15,000*g* for 5 min at 4°C. The final protein concentration was measured with BCA Protein Assay kit (Pierce, Rockford, IL). The proteins were denatured at 40°C for 45 min, separated by 7.5% SDS-polyacrylamide gel electrophoresis, transferred to a polyvinylidene difluoride membrane (Millipore, Billerica, MA), and then blotted for 1 h with rabbit anti-mouse PEPT1 antisera (raised against the COOH-terminal region, KGIGKENPYSSLEPVSQTNM, amino acids 690–709; Lampire Biological Laboratories, Inc., Pipersville, PA) (1:3000) (Hu et al., 2008). The membrane was washed three times with Tris-buffered saline and Tween 20 and then incubated with a secondary antibody, goat anti-rabbit

IgG conjugated to horseradish peroxidase (HRP) (Bio-Rad, Hercules, CA) (1:1000), for 1 h. For β-actin, the membrane was blotted with a mouse monoclonal antibody (Santa Cruz Biotechnology, Santa Cruz, CA) (1:1000) followed by the secondary antibody, goat anti-mouse IgG conjugated to HRP (Santa Cruz Biotechnology) (1:1000). The membranes were then washed five times with TBS-T buffer, and bound antibody was detected with Immobilon Western Chemiluminescent HRP Substrate (Millipore).

**Data Analysis.** The effective permeability ($P_{eff}$) was determined from the steady-state loss of drug from the perfusate as it flows through the intestine, according to a complete radial mixing (parallel tube) model (Komiya et al., 1980; Kou et al., 1991).

$$P_{eff} = \frac{-Q \cdot \ln(C_{out}/C_{in})}{2\pi RL} \quad (1)$$

In eq. 1, Q is the perfusate flow rate, R is the intestinal radius (0.1 cm), L is the length of intestine, $C_{in}$ is the inlet drug concentration, and $C_{out}$ is the outlet drug concentration (corrected for water flux). Preliminary studies indicated that [$^3$H]GlySar was stable in outlet perfusate samples, as determined by high-performance liquid chromatography with radiochemical detection (Ocheltree et al., 2005), thereby alleviating the need for additional corrections to $C_{out}$. In our studies, steady-state was reached at 20 to 30 min after the start of perfusion. The steady-state flux ($J$) across the intestinal membrane was then used to determine the kinetic parameters ($V_{max}'$ and $K_m'$) when referenced to inlet drug concentrations ($C_{in}$) as shown in eq. 2.

$$J = \frac{V_{max}' \cdot C_{in}}{K_m' + C_{in}} \quad (2)$$

Parameter estimates ($V_{max}$ and $K_m$) were also determined after factoring out the resistance across the unstirred water layer (i.e., using a modified boundary layer analysis) (Johnson and Amidon, 1988), and the steady-state flux ($J$) was referenced to intestinal wall concentrations ($C_w$) as shown in eq. 3.

$$J = \frac{V_{max} \cdot C_w}{K_m + C_w} \quad (3)$$

The relationship between intestinal wall and inlet drug concentrations is shown in eq. 4, where $P_{aq}$ is the unstirred aqueous layer permeability.

$$C_w = C_{in}\left(1 - \frac{P_{eff}}{P_{aq}}\right) \quad (4)$$

The unstirred aqueous layer permeability was determined according to eqs. 5 and 6:

$$P_{aq} = \left(A\frac{R}{D}Gz^{1/3}\right)^{-1} \quad (5)$$

$$Gz = \frac{\pi DL}{2Q} \quad (6)$$

where $D$ is the aqueous diffusion coefficient ($6.60 \times 10^{-4}$ cm$^2$/min), calculated according to the Hayduk-Laudie expression (Reid et al., 1977), Gz is the Graetz number (0.0829), and A is a unitless constant (1.332) estimated by A = 2.5 Gz + 1.125.

The flux eqs. 2 and 3 were modeled using a single saturable process (i.e., Michaelis-Menten), where $V_{max}'$ (or $V_{max}$) is the maximal flux and $K_m'$ (or $K_m$) is the Michaelis constant. The unknown kinetic parameters were then estimated by nonlinear regression. Other models, such as a single saturable process plus linear term and two saturable processes, were evaluated but did not improve the fit.

**Statistical Analysis.** Data were reported as mean ± S.E. A two-tailed Student's $t$ test was used to compare statistical differences between two groups. For multiple comparisons, one-way analysis of variance was used followed by Dunnett's test for pairwise comparisons with the control group (GraphPad Prism 4.0; GraphPad Software, Inc., La Jolla, CA). A probability of $p \leq 0.05$ was considered significant. Nonlinear regression analyses were performed using GraphPad Prism software, where the quality of fit was determined by evaluating the coefficient of determination ($r^2$), the S.E. of parameter estimates, and by visual inspection of the residuals.

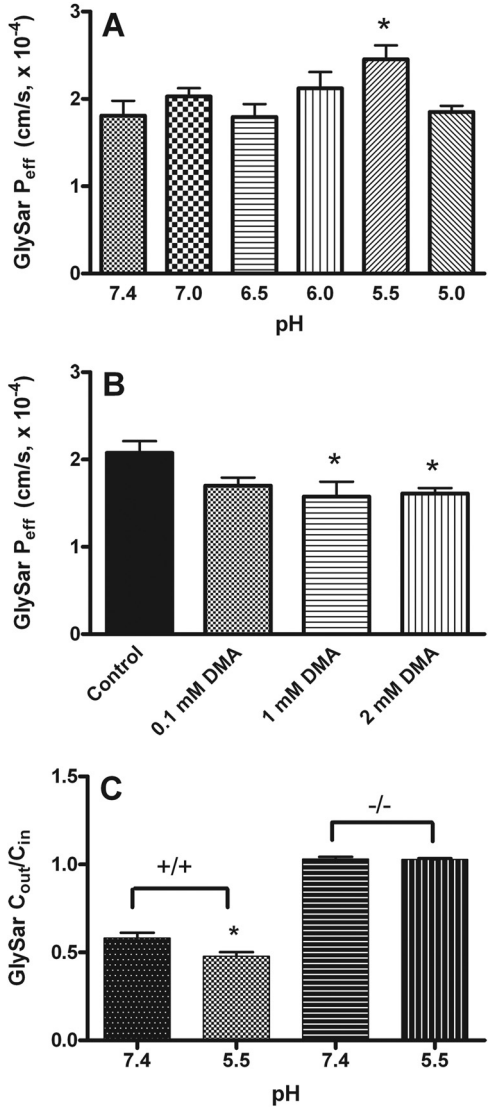


FIG. 1. Effect of pH (A) and DMA (in pH 6.5 buffer) (B) on the $P_{eff}$ of 10 μM [$^3$H]GlySar during jejunal perfusions of wild-type mice, *, $p \leq 0.05$ compared to pH 7.4 (A) or control values (B); effect of pH on the permeability (expressed as $C_{out}/C_{in}$) of 10 μM [$^3$H]GlySar during jejunal perfusions of wild-type (+/+) and *Pept1* knockout (−/−) mice (C). Data are expressed as mean ± S.E. ($n$ = 4).

## Results

**pH-Dependent Studies.** The effective permeability of 10 μM [$^3$H]GlySar was evaluated at various pH values to examine the proton-dependent jejunal uptake of GlySar by PEPT1. As demonstrated in Fig. 1A, there was a minor but statistically significant influence of pH on GlySar permeability in wild-type mice, with the optimal uptake being at pH 5.5. To further examine this relationship, increasing concentrations of dimethylamiloride (DMA), a $Na^+/H^+$ exchange inhibitor (Arakawa and Hara, 1999; Mirossay et al., 1999), were added to perfusate containing GlySar to disrupt the naturally occurring proton gradient. As observed in Fig. 1B, DMA decreased the jejunal permeability of GlySar in wild-type mice in a dose-dependent manner. In contrast, pH had no effect on GlySar permeability in *Pept1* knockout mice compared to wild-type animals (Fig. 1C). These results demonstrate that the proton-coupled transport of GlySar by jejunal PEPT1 is stimulated in an acidic environment.

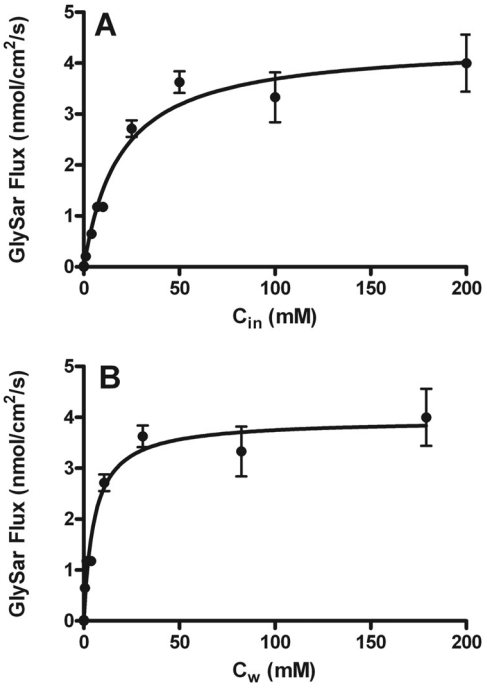


FIG. 2. Concentration-dependent flux of [$^3$H]GlySar (0.01–20 mM total substrate) during jejunal perfusions of wild-type mice. Studies were performed in pH 6.5 perfusion buffer. Data are expressed as mean ± S.E. ($n = 4$). $C_{in}$ represents the perfusate concentration of GlySar (A), whereas $C_w$ represents the mean "estimated" concentration of GlySar at the intestinal wall (B).

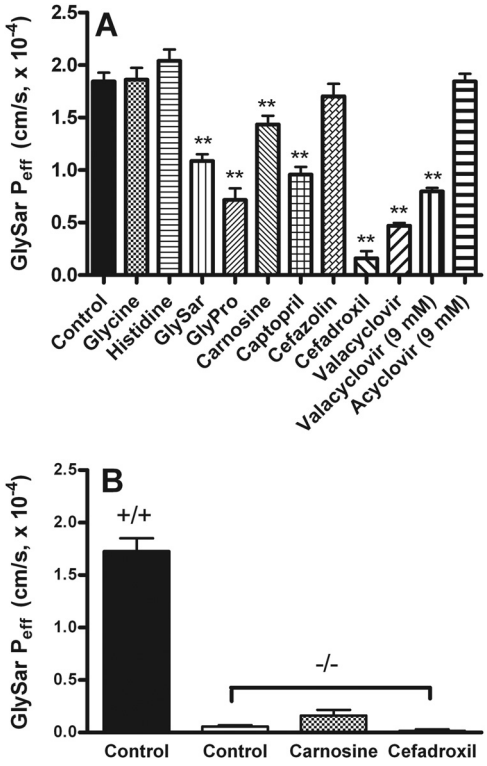


FIG. 3. Effect of potential inhibitors (25 mM except where noted) on the $P_{eff}$ of 10 $\mu$M [$^3$H]GlySar during jejunal perfusions of wild-type (+/+) mice (A) or *Pept1* knockout mice (−/−) (B). Studies were performed in pH 6.5 perfusion buffer. Data are expressed as mean ± S.E. ($n = 4$). **, $p \leq 0.01$ compared to control values.

**Concentration-Dependent Studies.** To determine the saturability of PEPT1 in jejunum, the uptake of [$^3$H]GlySar was evaluated at various concentrations of dipeptide (i.e., 0.01–200 mM total substrate in perfusate) in wild-type mice. As observed in Fig. 2A, GlySar exhibited a nonlinear flux that could be described by Michaelis-Menten kinetics, where $V_{max}' = 4.4 \pm 0.2$ nmol/cm$^2$/s and $K_m' = 19.8 \pm 3.3$ mM ($r^2 = 0.921$). When intestinal wall concentrations were used as a reference (i.e., adjusting for the unstirred water layer), the intrinsic absorption parameters were estimated as $V_{max} = 4.0 \pm 0.2$ nmol/cm$^2$/s and $K_m = 5.7 \pm 1.1$ mM ($r^2 = 0.916$) (Fig. 2B). These results demonstrate that GlySar was transported in a low-affinity manner, reflective of that for PEPT1.

**Inhibition Studies.** Specificity of the peptide-mediated uptake of 10 $\mu$M [$^3$H]GlySar was examined in mice by adding a wide range of potential inhibitors to the perfusate during jejunal perfusions. As depicted in Fig. 3A, GlySar permeability was significantly reduced in wild-type mice by several dipeptides (GlySar, GlyPro, and carnosine), the angiotensin-converting enzyme inhibitor captopril, the $\alpha$-amino-containing cephalosporin cefadroxil, and the antiviral prodrug valacyclovir. In contrast, the single amino acids glycine and histidine, the $\alpha$-amino-lacking cephalosporin cephazolin, and the active antiviral drug acyclovir had no effect. Likewise, carnosine and cefadroxil had no effect on the jejunal permeability of GlySar in *Pept1* knockout mice (Fig. 3B). Absence of GlySar inhibition by histidine, a known substrate for peptide/histidine transporters, suggested that PHT1/PHT2 were not involved in the intestinal permeability of this dipeptide.

**Regional Dependence for PEPT1 Activity.** To assess whether differences existed in the functional activity of PEPT1 along the intestine, GlySar permeability was evaluated in the small and large intestines of wild-type and *Pept1* knockout mice. As shown in Fig. 4, GlySar permeabilities were substantially lower in the duodenum, jejunum, and ileum of *Pept1* knockout mice compared to wild-type animals. In contrast, GlySar permeability was comparable between genotypes in mouse colon and was not any different between the intestinal segments of *Pept1* knockout mice. When GlySar permeabilities were compared among the intestinal segments of wild-type mice, dipeptide permeabilities were comparable in duodenum and jejunum, whereas ileal permeability was ~54% of that in jejunal or duodenal segments. The permeability of GlySar in colon was only 6% of that observed in the jejunum or duodenum.

Specificity of PEPT1 was also evaluated in various segments of the intestine. As demonstrated in Fig. 5, coperfusion of GlyPro or cefadroxil substantially decreased the permeability of GlySar in duodenum [by 52% for cefadroxil ($p > 0.05$) and 68% for GlyPro], jejunum (by 72% for cefadroxil and 78% for GlyPro), and ileum (by 58% for cefadroxil and 89% for GlyPro), but not in colon. However, in the presence of histidine, GlySar permeability was unaltered in any of the

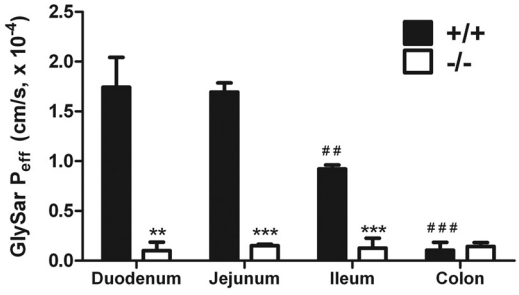


FIG. 4. $P_{eff}$ of 10 $\mu$M [$^3$H]GlySar in the duodenum, jejunum, ileum, and colon of wild-type (+/+) and *Pept1* knockout (−/−) mice. Studies were performed in pH 6.5 perfusion buffer. Data are expressed as mean ± S.E. ($n = 4$–8). ##, $p \leq 0.01$ and ###, $p \leq 0.001$ compared to both the duodenum and jejunum of wild-type mice; no differences were observed between the intestinal segments of *Pept1* knockout mice. **, $p \leq 0.01$ and ***, $p < 0.001$ when comparing *Pept1* knockout mice and wild-type animals for a specific intestinal segment.

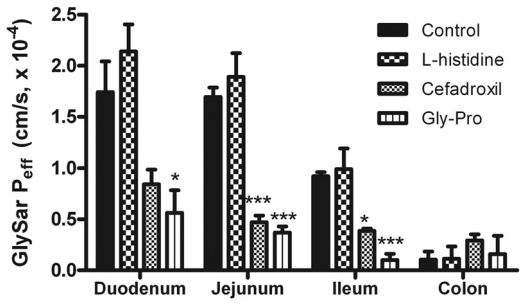


FIG. 5. Effect of potential inhibitors (25 mM) on the $P_{eff}$ of 10 $\mu$M [$^3$H]GlySar in the duodenum, jejunum, ileum, and colon of wild-type mice. Studies were performed in pH 6.5 perfusion buffer. Data are expressed as mean ± S.E. ($n$ = 4–8). *, $p \leq 0.05$ and ***, $p \leq 0.001$ compared to control values.

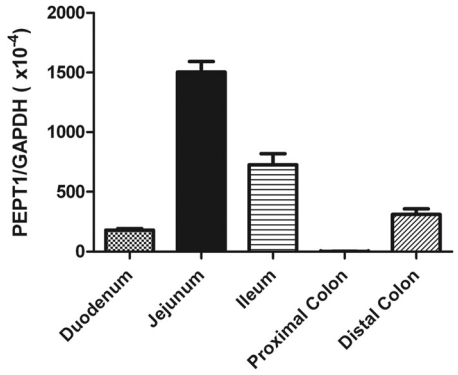


FIG. 6. Real time-PCR analyses for PEPT1 transcripts in the duodenum, jejunum, ileum, and proximal and distal colon of wild-type mice. Data are expressed as mean ± S.E. ($n$ = 6).

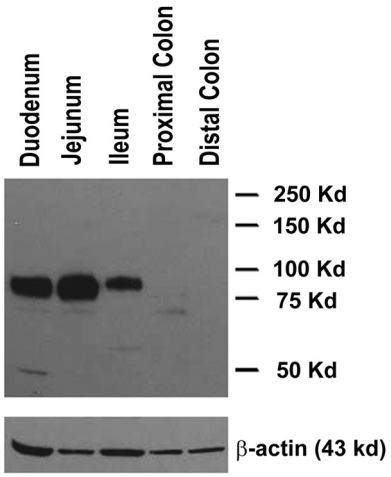


FIG. 7. PEPT1 protein expression in the duodenum, jejunum, ileum, and proximal and distal colon of wild-type mice. Tissue lysates from wild-type mice were subjected to 7.5% SDS-polyacrylamide gel electrophoresis (20 $\mu$g of protein per intestinal segment).

intestinal segments, demonstrating that PHT1/PHT2 was not involved in dipeptide uptake.

**Regional Dependence for PEPT1 Expression.** The functional activity of intestinal PEPT1 was confirmed by real-time PCR and immunoblot analyses. As shown in Fig. 6, the highest expression of PEPT1 transcripts was found in the jejunum followed by ileum, distal colon, duodenum, and proximal colon. When evaluated at the protein level (Fig. 7), the strongest staining of PEPT1 was found in jejunum followed by duodenum ≈ ileum. No PEPT1 protein was detected in the colon. It is interesting to note that although PEPT1 transcripts were found in distal colon, it did not translate to PEPT1 protein expression in this segment.

## Discussion

The recent generation of *Pept1* knockout mice has provided a unique opportunity to probe the functional activity of PEPT1 under physiological conditions (Hu et al., 2008). Although these authors examined the in situ permeability of GlySar from intestine, their phenotypic analysis was more preliminary in nature. In particular, they only evaluated GlySar at a single concentration and pH value, and permeability was evaluated in jejunal tissue alone as was PEPT1 protein. Other intestinal regions of the mice were neither examined for PEPT1 functional activity nor protein expression. Because of these limitations, we combined in situ permeability studies of GlySar and immunoblot analyses to compare dipeptide transport with PEPT1 protein expression in specific regions of the small intestine and colon.

In this study, we report several new findings regarding the in situ transport properties of GlySar in wild-type versus *Pept1* knockout mice and further validate these mice as a model to explore PEPT1 physiology and pharmacology. In particular, we found the following: 1) jejunal permeability of GlySar was saturable in wild-type mice with a low-affinity $Km$ = 5.7 mM; 2) GlySar permeability was specific for PEPT1; 3) functional activity of PEPT1 was highest in wild-type duodenum ≈ jejunum > ileum, with abundant protein expression in these same intestinal regions; 4) PEPT1 was not functionally active in the colon, which is consistent with its lack of protein expression in wild-type proximal or distal colon; 5) GlySar permeabilities were not different among the intestinal segments of *Pept1* null mice; and 6) residual uptake of GlySar was less than 10% in duodenum (or jejunum) when comparing *Pept1* null to wild-type animals. Taken as a whole, our studies show that PEPT1 has substantial activity along the entire length of mouse small intestine (but not colon), and that dipeptide permeability agrees with the expression levels of PEPT1 protein in these regions.

The pH-dependent transport activity of PEPT1 has been demonstrated in a variety of in vitro models, including rabbit intestinal brush border membrane vesicles (Ganapathy and Leibach, 1983; Ganapathy et al., 1984; Inui et al., 1988), Xenopus oocytes expressing rabbit (Fei et al., 1994), rat (Saito et al., 1995), human (Liang et al., 1995) and mouse (Fei et al., 2000) PEPT1, and cultured Caco-2 cells (Matsumoto et al., 1994; Terada et al., 1999). As shown in these studies, and when stably transfected in Chinese hamster ovary cells (Fujisawa et al., 2006), PEPT1 transport activity versus medium pH displayed a bell-shaped curve with an uptake maximum at pH 5.5 to 6.0. In our in situ studies, GlySar permeability was significantly greater at pH 5.5 (see Fig. 1A). However, the difference (approximately 36%) was not as remarkable as typically observed in other in vitro models. This result is most likely due to fact that changes in luminal bulk pH do not translate into similar changes in pH at the membrane surface of intact animals where the "acid-microclimate" is maintained during in situ or in vivo conditions (Lucas 1983). As shown by Högerle and Winne (1983), the microclimate jejunal pH varied from only 6.0 to 6.5 at the membrane surface even when the luminal bulk pH was raised from 5.0 to 7.4. Still, the pH dependence of PEPT1 activity was confirmed by our studies with DMA (see Fig. 1B), which presumably interfered with the ability of $Na^+/H^+$ exchanger 3 to acidify the luminal microclimate (Brandsch et al., 2008; Rubio-Aliaga and Daniel, 2008), thereby reducing the intestinal permeability of GlySar.

Human and mouse PEPT1 share many similarities, suggesting that our findings in mice should be relevant in predicting PEPT1-mediated processes in humans. At the molecular level, PEPT1 is highly homologous across species, having an amino acid identity of 83% between

humans (Liang et al., 1995) and mice (Fei et al., 2000). The genomic organization of human PEPT1 also shows high similarity with its mouse ortholog (Urtti et al., 2001). Functionally, as demonstrated in Xenopus oocytes or cell cultures, the transport properties of human and mouse PEPT1 are similar with respect to driving forces (i.e., stimulated by proton gradient and inside-negative membrane potential), substrate specificity, and substrate affinity (Liang et al., 1995; Fei et al., 2000). In regard to expression, PEPT1 is found in the small intestine and kidney of both species (Liang et al., 1995; Liu et al., 1995; Fei et al., 2000; Shen et al., 2003; Hu et al., 2008). Immunolocalization studies further place PEPT1 at the apical membrane of small intestine (i.e., duodenum, jejunum, and ileum), with little or no expression in the colon of humans and mice (Walker et al., 1998; Groneberg et al., 2001; Ford et al., 2003). Finally, gene expression studies show that both species have comparative intestinal expression patterns and levels, unlike that of the rat (Kim et al., 2007; Rubio-Aliaga and Daniel, 2008).

PEPT1 is a low-affinity, high-capacity transporter with apparent affinities ($K_m$ values) ranging from 0.2 to 10 mM, depending upon the substrate, species, tissue cell types, and experimental conditions such as buffer pH (Rubio-Aliaga and Daniel, 2002; Brandsch et al., 2008). The apparent affinity constants of GlySar are in the medium range of substrates, with $K_m$ values of approximately 0.5 to 1.5 mM. Under our conditions of study (i.e., in situ single-pass jejunal perfusion in mice), the intrinsic $K_m$ of GlySar was estimated at 5.7 mM. This value is similar to other PEPT1 substrates, namely cefadroxil, cephalexin, and cephradine, where the intrinsic $K_m$ values were 5.9, 7.2, and 1.5 mM, respectively, using an in situ single-pass jejunal perfusion technique in rats (Sinko and Amidon, 1988). In both studies (this study and that of Sinko and Amidon, 1988), these $K_m$ values are "unbiased" membrane parameters that have already factored out resistance across the unstirred aqueous boundary layer. In contrast, the $K_m$ of GlySar in mouse PEPT1 cRNA-injected Xenopus oocytes was approximately 0.7 mM at −50 mV (Fei et al., 2000). The apparent discrepancy between the two GlySar studies probably reflects differences in experimental design in which one study used an in vitro model (i.e., Xenopus oocytes) lacking in both blood flow and luminal residence times, whereas another study (this one) used a more physiologically based in situ intestinal perfusion model in mice.

Digestion of proteins in the intestinal lumen may yield di-/tripeptide concentrations as high as 100 mM (Ganapathy et al., 2006). Thus, having a low-affinity, high-capacity transporter such as PEPT1 in this region makes physiological sense. As observed in the current study, having a greater PEPT1 activity in the duodenum and jejunum over ileum is also physiologically sound because this POT protein has a reciprocal relationship with both peptidases and amino acid transporters along the small intestine. As the luminal contents move from the proximal to distal small intestine, the concentrations of di-/tripeptides gradually decrease and the concentrations of free amino acids gradually increase, thereby enhancing the efficiency of nutritive absorption.

Previous in vitro studies have shown that human PEPT1, in addition to recognizing di-/tripeptides, also recognizes peptidomimetic therapeutic agents such as captopril, aminocephalosporin antibiotics, and the antiviral prodrug valacyclovir (Brandsch et al., 2008; Rubio-Aliaga and Daniel, 2008). Our findings, using an in situ mouse intestinal perfusion model, were consistent with those studies regarding the substrate specificities of PEPT1. It is important to note that histidine, a known PHT1/PHT2 substrate, did not inhibit the permeability of GlySar in duodenal, jejunal, ileal, or colonic segments. This finding demonstrates that, despite their presence, the peptide/histidine transporters do not contribute to GlySar's uptake from the small and large intestines. It has already been confirmed that in *Pept1* null nice, other intestinal POT transporters, such as PEPT2, PHT1, and PHT2, do not exhibit a compensatory up-regulation in response to *Pept1* gene deletion (Hu et al., 2008).

In conclusion, our study provides the first comprehensive evaluation of the role, relevance, and regional dependence of PEPT1 expression and function in mouse intestines. The results demonstrate that PEPT1 protein is abundantly expressed along the entire length of small intestine with no expression in colon. The expression levels are corroborated by substantial PEPT1 activity in these same intestinal regions, as judged by GlySar permeability estimates during in situ single-pass perfusions. In comparing wild-type and *Pept1* knockout mice, it is clear that PEPT1 deficiency (e.g., a loss of activity due to polymorphisms, disease, or drug interactions) should have a major effect in reducing the intestinal absorption di-/tripeptides, peptidomimetics, and peptide-like drugs. Further studies with clinically relevant drugs (and prodrugs) are warranted and currently underway.

## References


Adachi Y, Suzuki H, and Sugiyama Y (2003) Quantitative evaluation of the function of small intestinal P-glycoprotein: comparative studies between in situ and in vitro. *Pharm Res* **20:**1163–1169.

Arakawa J and Hara A (1999) Effect of 5-(N,N-dimethyl)-amiloride, a specific inhibitor of Na(+)/H(+) exchanger, on the palmitoyl-L-carnitine-induced mechanical and metabolic derangements in the isolated perfused rat heart. *Pharmacology* **59:**239–248.

Bhardwaj RK, Herrera-Ruiz D, Eltoukhy N, Saad M, and Knipp GT (2006) The functional evaluation of human peptide/histidine transporter 1 (hPHT1) in transiently transfected COS-7 cells. *Eur J Pharm Sci* **27:**533–542.

Brandsch M, Knütter I, and Bosse-Doenecke E (2008) Pharmaceutical and pharmacological importance of peptide transporters. *J Pharm Pharmacol* **60:**543–585.

Daniel H and Rubio-Aliaga I (2003) An update on renal peptide transporters. *Am J Physiol Renal Physiol* **284:**F885–F892.

Daniel H and Kottra G (2004) The proton oligopeptide cotransporter family SLC15 in physiology and pharmacology. *Pflugers Arch* **447:**610–618.

Fei YJ, Kanai Y, Nussberger S, Ganapathy V, Leibach FH, Romero MF, Singh SK, Boron WF, and Hediger MA (1994) Expression cloning of a mammalian proton-coupled oligopeptide transporter. *Nature* **368:**563–566.

Fei YJ, Sugawara M, Liu JC, Li HW, Ganapathy V, Ganapathy ME, and Leibach FH (2000) cDNA structure, genomic organization, and promoter analysis of the mouse intestinal peptide transporter PEPT1. *Biochim Biophys Acta* **1492:**145–154.

Ford D, Howard A, and Hirst BH (2003) Expression of the peptide transporter hPepT1 in human colon: a potential route for colonic protein nitrogen and drug absorption. *Histochem Cell Biol* **119:**37–43.

Fujisawa Y, Tateoka R, Nara T, Kamo N, Taira T, and Miyauchi S (2006) The extracellular pH dependency of transport activity by human oligopeptide transporter 1 (hPEPT1) expressed stably in Chinese hamster ovary (CHO) cells: a reason for the bell-shaped activity versus pH. *Biol Pharm Bull* **29:**997–1005.

Ganapathy V and Leibach FH (1983) Role of pH gradient and membrane potential in dipeptide transport in intestinal and renal brush-border membrane vesicles from the rabbit. Studies with L-carnosine and glycyl-L-proline. *J Biol Chem* **258:**14189–14192.

Ganapathy V, Burckhardt G, and Leibach FH (1984) Characteristics of glycylsarcosine transport in rabbit intestinal brush-border membrane vesicles. *J Biol Chem* **259:**8954–8959.

Ganapathy V, Gupta N, and Martindale RG (2006) Protein digestion and absorption, in *Physiology of the Gastrointestinal Tract*, 4th edition (Johnson LR ed) pp 1667–1692, Elsevier, Burlington.

Groneberg DA, Döring F, Eynott PR, Fischer A, and Daniel H (2001) Intestinal peptide transport: ex vivo uptake studies and localization of peptide carrier PEPT1. *Am J Physiol Gastrointest Liver Physiol* **281:**G697–G704.

Herrera-Ruiz D, Wang Q, Gudmundsson OS, Cook TJ, Smith RL, Faria TN, and Knipp GT (2001) Spatial expression patterns of peptide transporters in the human and rat gastrointestinal tracts, Caco-2 in vitro cell culture model, and multiple human tissues. *AAPS PharmSci* **3:**E9.

Herrera-Ruiz D and Knipp GT (2003) Current perspectives on established and putative mammalian oligopeptide transporters. *J Pharm Sci* **92:**691–714.

Högerle ML and Winne D (1983) Drug absorption by the rat jejunum perfused in situ. Dissociation from the pH-partition theory and role of microclimate-pH and unstirred layer. *Naunyn Schmiedebergs Arch Pharmacol* **322:**249–255.

Hu Y, Smith DE, Ma K, Jappar D, Thomas W, and Hillgren KM (2008) Targeted disruption of peptide transporter *Pept1* gene in mice significantly reduces dipeptide absorption in intestine. *Mol Pharm* **5:**1122–1130.

Inui K, Okano T, Maegawa H, Kato M, Takano M, and Hori R (1988) H+ coupled transport of p.o. cephalosporins via dipeptide carriers in rabbit intestinal brush-border membranes: difference of transport characteristics between cefixime and cephradine. *J Pharmacol Exp Ther* **247:**235–241.

Institute of Laboratory Animal Resources (1996) *Guide for the Care and Use of Laboratory Animals* 7th ed. Institute of Laboratory Animal Resources, Commission on Life Sciences, National Research Council, Washington DC.

Jeong EJ, Liu Y, Lin H, and Hu M (2004) In situ single-pass perfused rat intestinal model for absorption and metabolism, in *Methods in Pharmacology and Toxicology Optimization in Drug Discovery: In Vitro Methods* (Yan Z and Caldwell GW eds) pp 65–76, Humana Press Inc, Totowa.

Johnson DA and Amidon GL (1988) Determination of intrinsic membrane transport parameters from perfused intestine experiments: a boundary layer approach to estimating the aqueous and unbiased membrane permeabilities. *J Theor Biol* **131:**93–106.

Kim HR, Park SW, Cho HJ, Chae KA, Sung JM, Kim JS, Landowski CP, Sun D, Abd El-Aty AM, Amidon GL, et al. (2007) Comparative gene expression profiles of intestinal transporters in mice, rats and humans. *Pharmacol Res* **56:**224–236.

Komiya I, Park JY, Kamani A, Ho NFH, and Higuchi WI (1980) Quantitative mechanistic studies in simultaneous fluid flow and intestinal absorption using steroids as model solutes. *Int J Pharm* **4:**249–262.

Kou JH, Fleisher D, and Amidon GL (1991) Calculation of the aqueous diffusion layer resistance for absorption in a tube: application to intestinal membrane permeability determination. *Pharm Res* **8:**298–305.

Liang R, Fei YJ, Prasad PD, Ramamoorthy S, Han H, Yang-Feng TL, Hediger MA, Ganapathy V, and Leibach FH (1995) Human intestinal $H^+$/peptide cotransporter. Cloning, functional expression, and chromosomal localization. *J Biol Chem* **270:**6456–6463.

Liu W, Liang R, Ramamoorthy S, Fei YJ, Ganapathy ME, Hediger MA, Ganapathy V, and Leibach FH (1995) Molecular cloning of PEPT 2, a new member of the H+/peptide cotransporter family, from human kidney. *Biochim Biophys Acta* **1235:**461–466.

Lucas M (1983) Determination of acid surface pH *in vivo* in rat proximal jejunum. *Gut* **24:**734–739.

Matsumoto S, Saito H, and Inui K (1994) Transcellular transport of oral cephalosporins in human intestinal epithelial cells, Caco-2: interaction with dipeptide transport systems in apical and basolateral membranes. *J Pharmacol Exp Ther* **270:**498–504.

Mirossay L, Mirossay A, Kocisová E, Radváková I, Miskovský P, and Mojzis J (1999) Hypericin-induced phototoxicity of human leukemic cell line HL-60 is potentiated by omeprazole, an inhibitor of H+K+-ATPase and 5′-(N,N-dimethyl)-amiloride, an inhibitor of Na+/H+ exchanger. *Physiol Res* **48:**135–141.

Ocheltree SM, Shen H, Hu Y, Keep RF, and Smith DE (2005) Role and relevance of peptide transporter 2 (PEPT2) in the kidney and choroid plexus: in vivo studies with glycylsarcosine in wild-type and PEPT2 knockout mice. *J Pharmacol Exp Ther* **315:**240–247.

Reid RC, Prausnitz JM, and Sherwood TK (1977) *The Properties of Gases and Liquids*, 3rd edition, p 573, McGraw-Hill Book Company, New York.

Rubio-Aliaga I and Daniel H (2002) Mammalian peptide transporters as targets for drug delivery. *Trends Pharmacol Sci* **23:**434–440.

Rubio-Aliaga I and Daniel H (2008) Peptide transporters and their roles in physiological processes and drug disposition. *Xenobiotica* **38:**1022–1042.

Rühl A, Hoppe S, Frey I, Daniel H, and Schemann M (2005) Functional expression of the peptide transporter PEPT2 in the mammalian enteric nervous system. *J Comp Neurol* **490:**1–11.

Saito H, Okuda M, Terada T, Sasaki S, and Inui K (1995) Cloning and characterization of a rat H+/peptide cotransporter mediating absorption of beta-lactam antibiotics in the intestine and kidney. *J Pharmacol Exp Ther* **275:**1631–1637.

Shen H, Smith DE, Keep RF, Xiang J, and Brosius FC 3rd (2003) Targeted disruption of the PEPT2 gene markedly reduces dipeptide uptake in choroid plexus. *J Biol Chem* **278:**4786–4791.

Sinko PJ and Amidon GL (1988) Characterization of the oral absorption of beta-lactam antibiotics. I. Cephalosporins: determination of intrinsic membrane absorption parameters in the rat intestine in situ. *Pharm Res* **5:**645–650.

Terada T, Sawada K, Saito H, Hashimoto Y, and Inui K (1999) Functional characteristics of basolateral peptide transporter in the human intestinal cell line Caco-2. *Am J Physiol* **276:**G1435–G1441.

Urtti A, Johns SJ, and Sadée W (2001) Genomic structure of proton-coupled oligopeptide transporter hPEPT1 and pH-sensing regulatory splice variant. *AAPS PharmSci* **3:**E6.

Walker D, Thwaites DT, Simmons NL, Gilbert HJ, and Hirst BH (1998) Substrate upregulation of the human small intestinal peptide transporter, hPepT1. *J Physiol* **507:**697–706.

**Address correspondence to:** Dr. David E. Smith, Department of Pharmaceutical Sciences, University of Michigan, 4742 Medical Sciences II, 1150 W Medical Center Drive, Ann Arbor, MI 48109-5633. E-mail: smithb@umich.edu